Electrical Power Quality and Utilisation, Journal Vol. XI, No. 2, 2005

EMC Shielding in Power Electronics Multilayers

Stephan SCHUH, Manfred ALBACH
Friedrich-Alexander University of Erlangen-Nuremberg, Germany

Summary: **The integration of passive components in printed circuit boards by using structured layers of different material leads to completely new technical challenges, both in technological realisations and in simulations or modelling of the embedded components. The integration of inductive components is very interesting due to the substantial place reduction on the surface of the printed circuit board. In this context the shielding of the stray field of these inductive components leads to some new approaches in magnetic field calculation and simulation by planar structures. So in this paper the influence of FPC foils (Ferrite Polymer Compounds), m-metal and thin layers of copper on the magnetic field distribution and thus on the inductive coupling mechanisms in multilayers is analytically calculated and verified by some measurements. The presented results – measurement and simulation – lead to the final conclusion that the integration of ì-metal in comparison to FPC foils and thin layers of copper in the multilayer is one of the promising procedures for EMC-shielding.**

Key words:
power electronics, multilayer planar passive component, analytical analysis

1. INTRODUCTION

1.1. Multilayer technology

The trend towards flat designs of power electronic circuits has lead to different technical approaches. Whereas in the past designers mainly tried to reduce the height of passive components, one example are the planar inductors and transformers, a new trend towards integrating the functionality of passive components can be observed.

An increasing miniaturization of PCB-based circuits can be achieved through the constant research in SMD-technology. The integration of passive components in this concept is not possible in parts or in general. As these components need more than 2/3 of the space of a conventional circuit [7] the potential for miniaturization is very high. The integration of passive components in the substrate of the circuit by using layered structures and materials with dielectric and magnetic characteristics is one of the possibilities. A so-called multilayer is developed, e.g. the emPIC circuit (*em*bedded *p*assives *i*ntegrated *c*ircuits) [7] deals with this concept. This technology is highly attractive to the automation process and the level of repeatability from part-to-part also improves.

In [8] the principle of the embedded passives integrated circuit together with the expected advantages is presented. The integration of the passive components in the PCB makes the circuit compact and thin by removing the space between the components, considerably. It also reduces the conventional component count, eliminates solder joints, and provides low electromagnetic interference solutions.

Figure 1 shows a realised converter with pcb-integrated planar inductive components. The whole circuit is much thinner than a conventional converter.

For a better understanding in Figure 2 model for the same converter is given in a schematic form.

On the other hand, the combination of integration technologies and functionally integrated devices not only leads to very compact and ultra thin circuits, but also to a number of various new technical challenges. This includes both, the fabrication process (hardware) as well as the understanding of the circuit behaviour, this means the design and simulation of such a circuit (software). The components can no longer be treated as discrete components, because of the capacitive and inductive coupling mechanisms between the adjacent components. If the well known circuit simulators should be used for this type of integrated passive components, a considerably improved modelling of these 3-dimensional structures (see Fig. 3) becomes now necessary.

This paper deals with some important aspects of the magnetic devices and the EMC-shielding of the stray fields of these devices. The first important issue is the decoupling of the different current loops on the various layers in these extremely compact components, this means that the screening

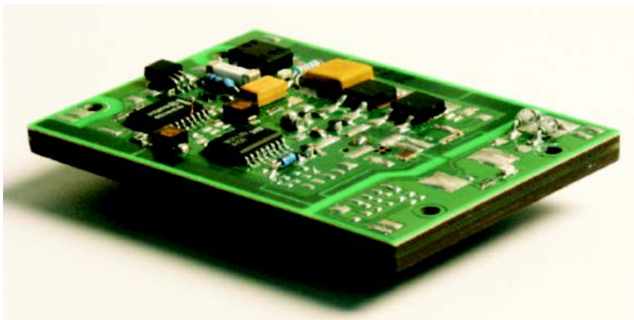

Fig. 1. Converter with integrated inductive components in the substrate

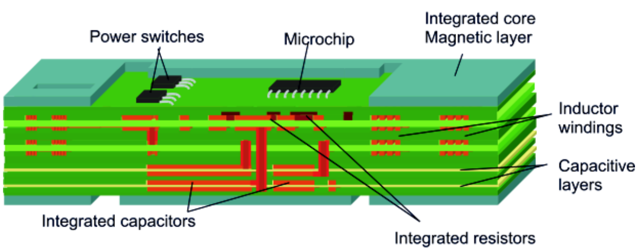

Fig. 2. emPIC converter model

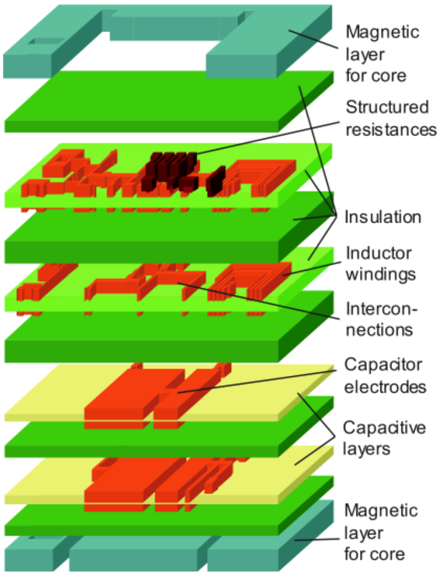

Fig. 3. 3-dimensional converter model

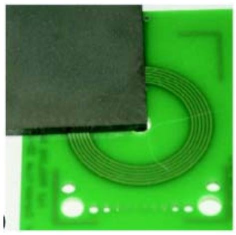

Fig. 4. Planar spiral winding with soft magnetic core

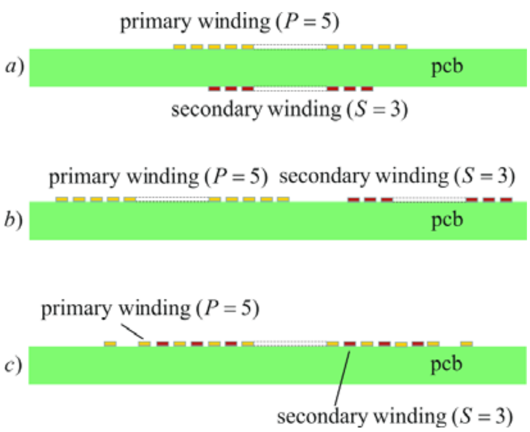

Fig. 5. Transformer designs

effectiveness of the conductive and permeable layers has to be investigated. If transformers are realised with planar spiral windings, the coupling between primary and secondary windings is another important issue. Last but not least the screening of the whole magnetic field caused by such a multilayer is also interesting for EMC standardization and inspection.

So on the following pages the influence of FPC foils, m-metal and thin layers of copper on the magnetic flux density is investigated. This then forms the basis for any further calculations like coupling of circuits and screening between different layers.

1.2. Inductive components

Integrated windings are state of the art. They are realised by means of spiral windings which are etched directly on the pcb. The self inductance can be even increased when they are located between thin magnetic layers. The realised spiral winding which is shown in Figure 4 is used for the calculations and measurements later on.

In addition to planar inductances pcb-based planar transformers are built in a multilayer, too. Some design possibilities are given in Figure 5.

Both best coupling between the primary and the secondary winding and minimal area needed by the windings is achieved with the interleaved configuration (see Fig. 5c). In consequence of the small distance between the secondary and the primary the interleaved configuration has only a minor disruptive strength.

Basically with the application of permeable material on both sides the achieved coupling is considerably higher and the stray field outside of the component is screened.

1.3. Materials

For the purposed EMC shielding two effects which are depending on material parameters are suitable.

Permeable material has a constant screening effect on magnetic fields over a wide range of operating frequencies. The losses inside the material are comparably low as long as the material does not saturate. One promising material class are ferrite polymer compounds (FPC). They consist of ferrite powder in a polymer matrix. The single particles of ferrite are insulated from each other by the plastic. Thus the material is nearly not conductive. The permeability of FPC materials is typically low in the range of $\mu_r = 10$ to 20. The used material for calculations and measurements in this paper has a permeability of $\mu_r = 11$ with thickness $d = 200\mu$m.

A shielding effect is reached by conductive material, too. The eddy currents inside the material caused by the external magnetic field reduce the magnetic field outside the circuit. But the losses are considerably higher. μ-metal foils combine these two effects described before. μ-metal is an amorphous alloy which has in comparison with FPC-material a much higher permeability. Consequently, a much higher screening or shielding effect of the final multilayer is obtained. However, due to the non negligible conductivity of the μ-metal foils, the eddy currents inside the material enlarges the effect. Thus the challenge is to develop an analytical model, which takes the conductivity σ and the permeability into account. All calculations and measurements presented in the figures in this paper are made with layers of μ-metal with the following parameters: $\mu = 4000 \cdot \mu_0$, $\sigma = 1.8 \cdot 10^6 \Omega\text{m}^{-1}$ and layer thickness $d = 50\mu$m. Both materials are shown in Figure 6.

2. ANALYTICAL ANALYSIS

2.1. Simplified model

Figure 7 shows two schematic diagrams as initial point for the analytical research. In both pictures a circular circuit path is given as a symmetrically current film $\underline{K}_{er}$ around the origin of a coordinate system. Later on every turn of the given planar coil is represented by a single current film. The increasing radius of the spiral winding and the interconnections between the single tracks are neglected for the analytical analysis. One or two planar conductive and/or permeable layers are placed in a parallel direction to the current film at distance b_2 or b_5.

All calculations are done with the magnetic vector potential in the following equations. Due to the induced eddy currents with angular frequency ω the complex form of the magnetic vector potential $\underline{\vec{\mathbf{A}}}$ is used. If $\underline{\vec{\mathbf{A}}}$ is known in the whole area the related magnetic field strength $\underline{\vec{\mathbf{H}}}$, the magnetic flux density $\underline{\vec{\mathbf{B}}}$ and the current density $\underline{\vec{\mathbf{J}}}$ can be determined with:

$$\underline{\vec{\mathbf{H}}} = \frac{1}{\mu}\,\mathrm{rot}\,\underline{\vec{\mathbf{A}}} \tag{1}$$

$$\underline{\vec{\mathbf{B}}} = \mu \underline{\vec{\mathbf{H}}} \tag{2}$$

$$\underline{\vec{\mathbf{J}}} = -\mathrm{j}\omega\sigma \underline{\vec{\mathbf{A}}} \tag{3}$$

2.2. Boundary value problem

The influence on the magnetic vector potential $\underline{\vec{\mathbf{A}}} = \vec{\mathbf{e}}_\varphi \underline{A}(\rho,z)$ by the conductive and/or permeable layers can be calculated by solving a boundary value problem. This methodology is well known, nevertheless, the basic equations for this mathematical procedure are described in the following. Some more detailed information to the procedure are given in [4] and [5].

For the situations given in Figure 7 in every region with different permeability μ and/or conductivity σ the skin equation:

$$\mathrm{rot}\ \ \mathrm{rot}\ \ \underline{\vec{\mathbf{A}}} + \alpha^2\ \ \underline{\vec{\mathbf{A}}} = \vec{\mathbf{0}} \tag{4}$$

with:

$$\alpha^2 = j\,\omega\mu\sigma \tag{5}$$

has to be solved. The parameter α is zero outside the conductive-permeable material, where the skin equation simplifies to the Laplace equation:

$$\mathrm{rot}\ \ \mathrm{rot}\ \ \underline{\vec{\mathbf{A}}} = \vec{\mathbf{0}} \tag{6}$$

The general solution of this boundary value problem is obtained with the boundary conditions at z = 0 with the surface current distribution:

$$-\frac{1}{\mu_a}\frac{\partial \underline{A}_a}{\partial z}\bigg|_{z=z_i+} + \frac{1}{\mu_b}\frac{\partial \underline{A}_b}{\partial z}\bigg|_{z=z_i-} = \underline{K}_{er}(\rho) \tag{7}$$

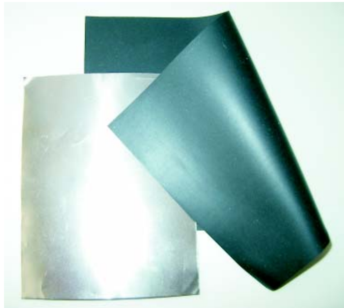

Fig. 6. μ-metal (silver) and FPC-material (black)

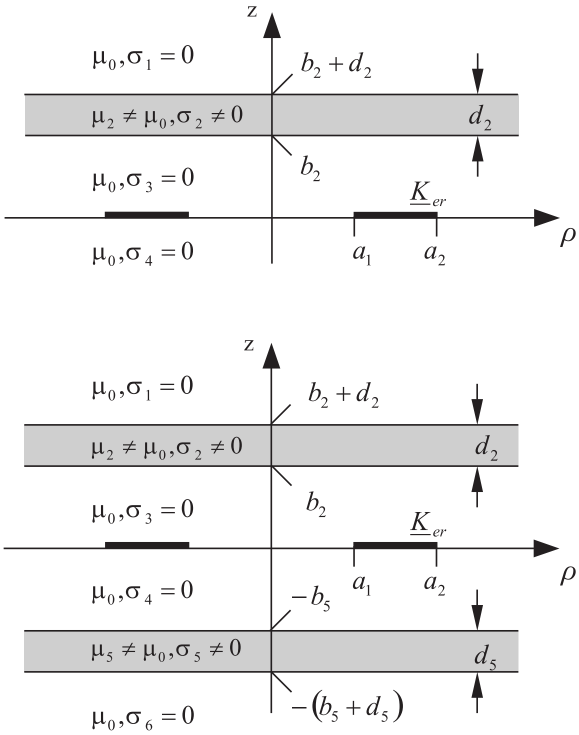

Fig. 7. Cross section for the boundary value problem

and furthermore with the requirement:

$$\vec{\mathbf{A}}(\rho, z \to \pm\infty) \to \vec{\mathbf{0}} \tag{8}$$

Finally the solution of each region is coupled with every other region by the boundary condition at both surfaces of the conductive-permeable layer:

$$\left(\frac{\partial \underline{A}_a}{\partial \rho} + \frac{\underline{A}_a}{\rho}\right)\bigg|_{z=z_i+} = \left(\frac{\partial \underline{A}_b}{\partial \rho} + \frac{\underline{A}_b}{\rho}\right)\bigg|_{z=z_i-} \tag{9}$$

Taking into account all this equations before the detailed determination of the magnetic vector potential in each region is possible. According to Figure 7 the results are four magnetic potentials ($\underline{\vec{\mathbf{A}}}_1$ to $\underline{\vec{\mathbf{A}}}_4$) in the case with one layer and two more ($\underline{\vec{\mathbf{A}}}_1$ to $\underline{\vec{\mathbf{A}}}_6$) by using two conductive-permeable layers – one separate magnetic vector potential for each region. The subscription is identical to the permeability and conductivity given in Figure 7.

Due to the fairly complex and extensive results of the obtained magnetic vector potential the final expressions are not presented here. They are from minor interest compared to the calculation and measurement results. Further details and additional results in this context will be found in [4] and [5].

2.3. Attenuation and self inductance

An inductive component is characterised primarily by the self inductance and the magnetic stray field in the vicinity. In comparison to a magnetic device without any permeable and/or conductible material in the vicinity the conductive-permeable layers in the multilayer close to the planar coil change the self inductance and the magnetic stray field of this component and the multilayer.

The interference of the stray field can be illustrated by regarding the attenuation of the magnetic field strength $\underline{\vec{\mathbf{H}}}$ outside of the whole component:

$$\frac{att}{\mathrm{dB}} = 20\,log\,\frac{\left|\underline{\vec{\mathbf{H}}}\right|_{\text{without any layer}}}{\left|\underline{\vec{\mathbf{H}}}\right|_{\text{with layer}}} \qquad (10)$$

While for the determination of the attenuation the vector potential outside the whole magnetic component is needed the self inductance can be calculated by using the magnetic flux density $\underline{\vec{\mathbf{B}}}$ in the region of the given planar coil. If this planar coil is realised by means of a spiral winding each turn may be treated as a single circular loop. The inductance of the complete spiral winding is obtained by assuming a current $\underline{I}$ through the winding, calculating the contribution of all turns to the flux density and then integrating this total flux density over the area of all turns. The inductance of a spiral winding consisting of N turns is then given by the relation:

$$L = \frac{1}{\underline{I}}\sum_{i=1}^{N}\underline{\Psi}_i \qquad (11)$$

with the magnetic flux:

$$\underline{\Psi}_i = \iint_{a_i}\underline{\vec{\mathbf{B}}}\cdot d\vec{\mathbf{a}} = \oint_{C_{a_i}}\underline{\vec{\mathbf{A}}}\cdot d\vec{\mathbf{s}} \qquad (12)$$

According to equation (12) the calculation of the magnetic flux $\underline{\Psi}_i$ through turn number i can be determined either by integrating the flux density $\underline{\vec{\mathbf{B}}}$ over the area a_i covered by turn number i or by integrating the vector potential $\underline{\vec{\mathbf{A}}}$ along the contour C of this turn. With equation (11) the self inductance of each turn and also the coupling between the turns is taken into consideration. The so-called inner inductance, representing the energy stored inside the copper winding is neglected in this equation.

For discussing the results of both calculations and measurements only the increase of the self inductance ΔL compared to an air-core coil:

$$L = L_{\text{air coil}} + \Delta L \qquad (13)$$

is displayed in the following figures.

3. RESULTS

3.1. Planar coil for analysis

For the measurements a special multilayer pcb has been used, where 4 layers with 6 turns per layer have been integrated inside the pcb. In fig. 8 a schematic configuration with all dimensions is given. This inductive component has been used because of the adequate large magnetic field strength caused by the overall 24 circular windings. For the final calculations all formulae given before for one circular winding with a current film $\underline{K}_{er}$ have to be adapted by easily summing up the contributions of each circular turn.

According to equation (13) the self inductance of this special multilayer without any conductive-permeable material in the vicinity is needed. The impedance $\underline{Z} = R + j\omega L$ is measured by an impedance analyser. With a frequency of $f = 100\mathrm{kHz}$ the measured self inductance of the air coil has a value of $L_{\text{air coil}} = 26\mu\mathrm{H}$. All measurements below are done by the same frequency.

3.2. Attenuation of magnetic field strength

First of all the attenuation of the magnetic field strength of an inductive component in a multilayer according to Figure 7 with one or two FPC-foils and a distance between foil and current loop $b_2 = b_5 = 1.6\mathrm{mm}$ is examined. As the ferrite powder is integrated in the plastic matrix the conductivity σ_2 and σ_5 of the FPC-foil are equal to zero, too. So there is no screening or shielding effect by eddy currents.

In Figure 9 the circular planar coil is represented easily by a right-hand orientated magnetic dipole shown as arrow in the origin. It can be seen that in the region behind the foil ($z > b + d$) the field amplitude (on the z-axes) is reduced by a maximum

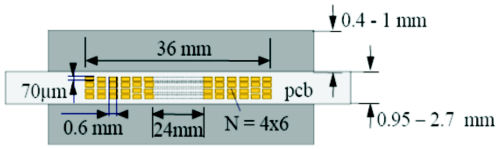

Fig. 8. Cross section of the inductive component

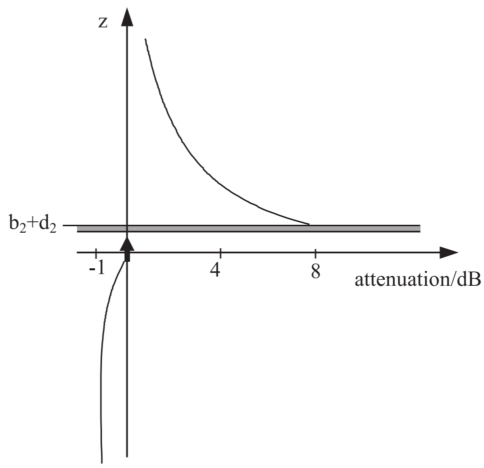

Fig. 9. Attenuation of the magnetic field strength on the z-axes with only one FPC-foil

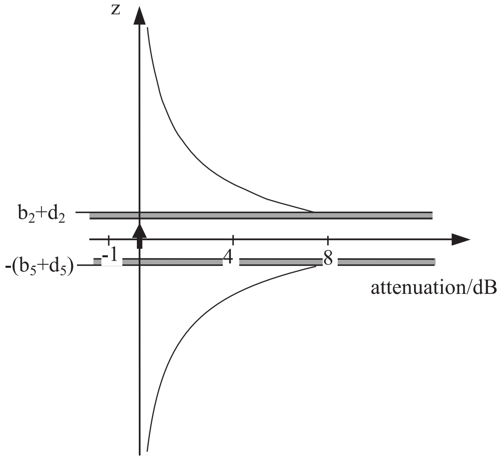

Fig. 10. Attenuation of the magnetic field strength on the z-axes with two FPC-foils

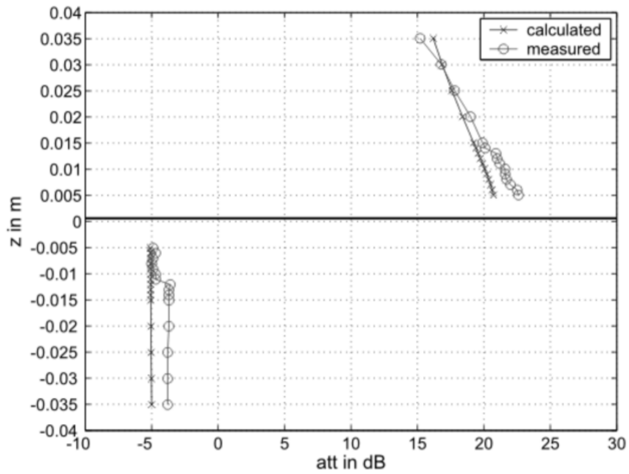

Fig. 11. Attenuation of magnetic field strength on the z-axes with only one μ-metal layer

value of less than 8dB. This value is only achieved close to the foil. At a larger distance the field attenuation becomes considerably smaller, which means, that the influence of the foil vanishes.

In the region z < 0 the attenuation becomes negative. Thus an amplification of the field is observed, which may leads to EMC problems.

The result for a comparable situation where the current loop is located in the middle between two identical FPC foils of the same thickness is shown in Figure 10. In this case now the field is reduced symmetrical on both sides. But the attenuation value at a given distance is generally smaller than in the case with only one FPC foil.

In both cases described above the screening effectiveness is relatively poor, which is mainly due to the low permeability.

In the next two figures (Fig. 11 and 12) below the results for a comparable situation as discussed before are given. Only the FPC foils are now changed to layers of μ-metal with a thickness of 50μm.

In case of one layer the attenuation behind the layer is more than doubled due to the contribution of the additional eddy currents in the conductive μ-metal. Comparing Figure 12 with Figure 10 the attenuation value is nearly the same but in the case of the μ-metal only with a fourth of material thickness.

Finally Figure 13 shows exactly the same situation as in the case with two μ-metal layers before but now with two layers of copper in the same thickness (conductivity of copper: $\sigma_2 = \sigma_5 = 58 \cdot 10^6 \Omega m^{-1}$). Due to the skin depth of about 200μm at 100kHz the attenuation is comparably poor.

3.3. Increase of self inductance

Conductive-permeable layers in a multilayer for EMC-shielding have not only a screening effect on the stray field outside the multilayer. They also have an influence on the self inductance of the component. For the same dimensions and multilayer structure as described in the first four cases in the chapter before the results for the increase of the self inductance are given next.

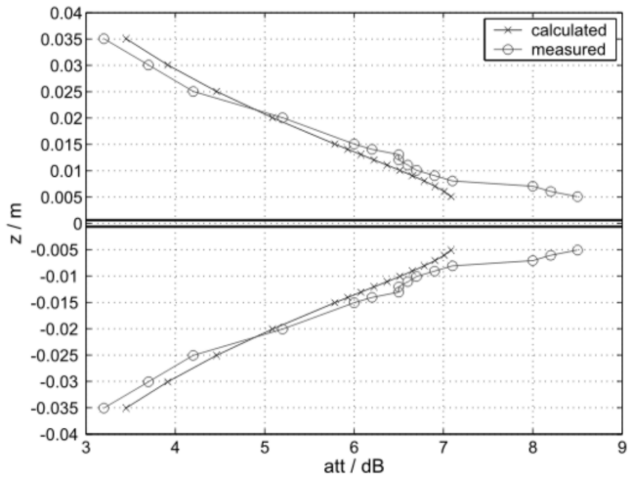

Fig. 12. Attenuation of magnetic field strength on the z-axes with two μ-metal layers

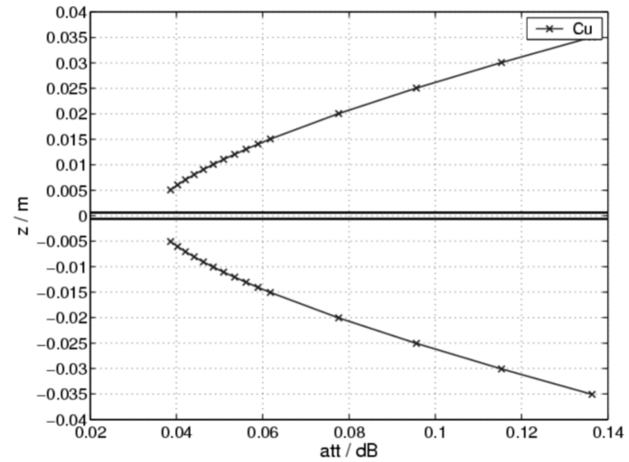

Fig. 13. Attenuation of magnetic field strength on the z-axes with two copper layers

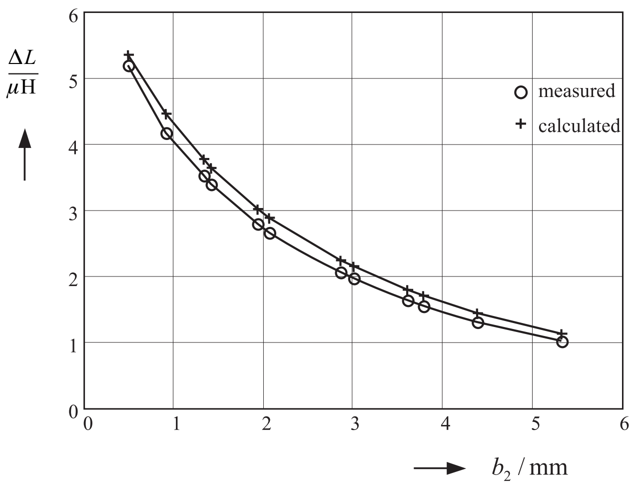

Fig. 14. Increase of the self inductance with only one FPC-foil

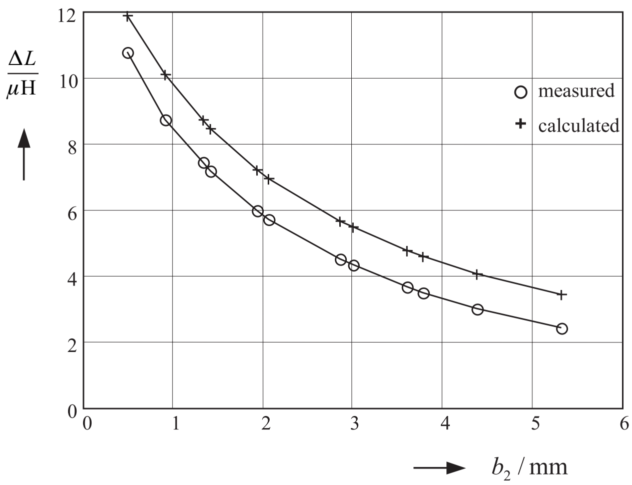

Fig. 15. Increase of the self inductance with two FPC-foils

The first result is given in Figure 14, where one FPC-foil has been used only on one side of the pcb. Increasing the distance reduces the influence of the foil and thus the increase of the inductance. The maximum increase of the inductance of 5μH compared to the original value of 26μH is comparably low.

With one FPC foil on each side of the planar inductive component the increase of the self inductance is , compared to the case with only one foil, now more than doubled as shown in Figure 15.

Finally Figure 16 shows the results for a device with one μ-metal layer in the vicinity of the inductive component. In that case the self inductance can be doubled nearly although only one μ-metal foil is used. If the distance between pcb and foil raises, the influence of the permeable and conductive material vanishes as seen before. Thus the self inductance converges to the value of the air coil. With two layers of μ-metal the self inductance of the planar coil can increase remarkably. In Figure 17 the 15-fold value of the air coil is reached.

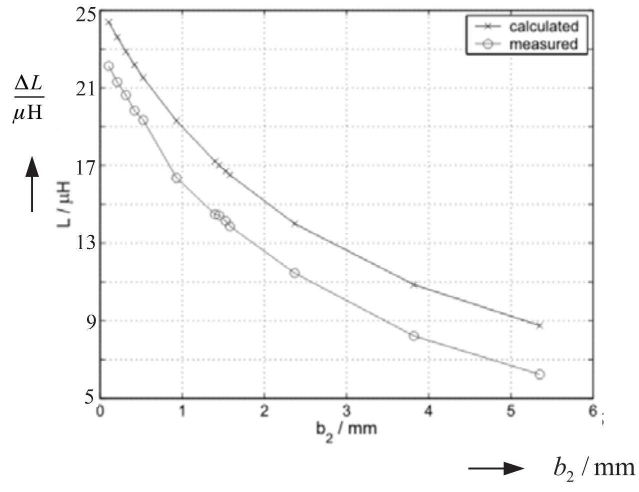

Fig. 16. Self inductance with only one μ-metal layer

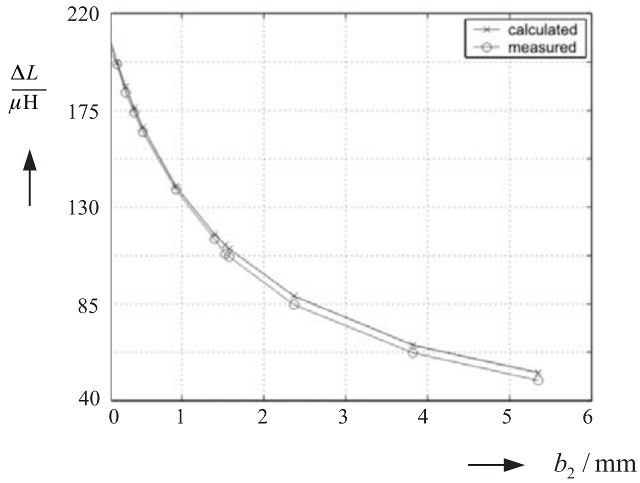

Fig. 17. Self inductance with two μ-metal layers

4. CONCLUSION

In the future the space reduction of classical inductive components becomes more and more important due to the needed miniaturisation in commercially used circuits. Planar inductive components which are integrated in multilayer structures are one of the promising concepts. Building these extremely compact components particular efforts have to be spend for the EMC-shielding of the stray fields outside and the magnetic coupling inside to avoid malfunctions of the whole components.

In this paper some general informations on multilayer structures and different materials for realising magnetic components are given. A calculation method for the determination of the magnetic vector potential in all regions of the multilayer is presented. With the knowledge of this potential the attenuation of the magnetic field strength outside the ciruit and the increase of the self inductance can easily be calculated. Both effects are caused by conductive-permeable layers in the vicinity of the inductive components.

Finally some simulation and measurement results give an impression of the influence on the magnetic field strength caused by permeable-conductive layers. The presented results lead to the conclusion that the integration of μ-metal in the multilayer is one of the promising procedures for EMC-shielding.

5. ACKNOWLEDEMENTS

This publication is based on the work of the consortium "3D-integration in power electronics" consisting of the partners Philips Research, Isola, Straschu, Ruwel and EMF at University Erlangen, all Germany, which was funded by the German government, Förderkennzeichen 01M3118A.

REFERENCES

1. Albach M., Schuh S.: *Analysis of embedded passives integrated circuits for power converters.* Power Conversion Intelligent Motion Conference – PCIM, Nuremberg, Germany, 2003.
2. Chen W., Yan Y., Hu Y.: *Model and design of PCB winding parallel for planar transformers.* IEEE International Magnetics Conference – INTERMAG, Boston, USA, 2003.
3. Faucher S., Joubert C., Forest F., Wilmot F., Labouré E., Costa F.: *Passive Components Integration for Power Electronic.* IEEE European Conference on Power Electronics and Applications – EPE, Leoben, Austria, 2001.
4. Schuh S., Albach M.: *Magnetic field distribution in embedded passive integrated circuits.* IEEE European Conference on Power Electronics and Applications – EPE, Toulouse, France, 2003.
5. Schuh S., Albach M., Koch R.: *Planar inductive components in the vicinity of conductive, permeable material.* Power Conversion Intelligent Motion Conference – PCIM, Nuremberg, Germany, 2005.
6. Waffenschmidt E., Ackermann B.: *Power converter with printed circuit board integrated passive components.* IEEE European Conference on Power Electronics and Applications – EPE, Toulouse, France, 2003.
7. Waffenschmidt E., Ferreira J.A.: *Embedded passives integrated circuits for power converters*. IEEE Power Electronics Specialists Conference – PESC, Cairns Australia, 2002.
8. Waffenschmidt E., Ackermann B., Langkabel E., Wille M., Marczinske H., Schuh S.: *Integral manufacturing of embedded passives integrated circuits for power electronics*. Power Conversion Intelligent Motion Conference – PCIM, Nuremberg, Germany, 2004.

Dipl.-Ing. Univ. Stephan Schuh

Stephan Schuh received the Diploma of Engineer degree at University Erlangen-Nuremberg in the year 2000. He has done his diploma thesis in the area of energy technology and drive engineering. Since 2001 he is a research scientist at the Chair of Electromagnetic Fields at University Erlangen-Nuremberg. S. Schuh is currently working toward the Doctorate degree in Electrical Engineering. His current research interests are problems in electrodynamics, electromagnetic compatibility and packaging in power electronics.

Address:
Chair of Electromagnetic Fields
Friedrich-Alexander-University Erlangen-Nuremberg
Cauerstrasse 7 - 91058 Erlangen; Germany
Telefon: +49 9131 8528949
Telefax: +49 9131 8527787
s.schuh@emf.eei.uni-erlangen.de

Prof. Dr.-Ing. Manfred Albach

Manfred Albach studied Electrotechnics at the Technical University Berlin and received the Ph.D. degree in the year 1983 with the subject of skin effect problems. From 1983 to 1999 he was a research scientist at Philips Research Laboratory in Aachen, Germany, in the area of investigations in power electronics with emphasis on EMC problems and magnetic components. Since 1999 he is Professor at the University Erlangen-Nuremberg, Germany and the head of the Chair of Electromagnetic Fields. M. Albach does research in the area of fundamental problems in electrodynamics, electromagnetic compatibility and magnetic components for high frequency and large signal applications. He is a member of the IEEE.

Address:
Chair of Electromagnetic Fields
Friedrich-Alexander-University Erlangen-Nuremberg
Cauerstrasse 7 - 91058 Erlangen, Germany
Telefon: +49 9131 8528953
Telefax: +49 9131 8527787
m.albach@emf.eei.uni-erlangen.de